



This is a repository copy of *Gamma irradiation resistance of an early age slag-based cement matrix for nuclear waste encapsulation*.

White Rose Research Online URL for this paper:

<http://eprints.whiterose.ac.uk/86429/>

Version: Accepted Version

---

**Article:**

Mobasher, N., Bernal Lopez, S., Kinoshita, H. et al. (2 more authors) (2015) Gamma irradiation resistance of an early age slag-based cement matrix for nuclear waste encapsulation. *Journal of Materials Research*, 9 (30). 1563 - 1571. ISSN 0884-2914

<https://doi.org/10.1557/jmr.2014.404>

---

**Reuse**

Unless indicated otherwise, fulltext items are protected by copyright with all rights reserved. The copyright exception in section 29 of the Copyright, Designs and Patents Act 1988 allows the making of a single copy solely for the purpose of non-commercial research or private study within the limits of fair dealing. The publisher or other rights-holder may allow further reproduction and re-use of this version - refer to the White Rose Research Online record for this item. Where records identify the publisher as the copyright holder, users can verify any specific terms of use on the publisher's website.

**Takedown**

If you consider content in White Rose Research Online to be in breach of UK law, please notify us by emailing [eprints@whiterose.ac.uk](mailto:eprints@whiterose.ac.uk) including the URL of the record and the reason for the withdrawal request.

## **Gamma irradiation resistance of an early age slag-based cement matrix for nuclear waste encapsulation**

Neda Mobasher<sup>1</sup>, Susan A. Bernal<sup>1</sup>, Hajime Kinoshita<sup>1</sup>, Clint A. Sharrad<sup>2</sup>, John L. Provis<sup>1\*</sup>

<sup>1</sup>Immobilisation Science Laboratory, Department of Materials Science & Engineering,  
The University of Sheffield, Sheffield S1 3JD, United Kingdom

<sup>2</sup>Research Centre for Radwaste and Decommissioning, Dalton Nuclear Institute,  
The University of Manchester, Oxford Road, Manchester M13 9PL, United Kingdom

\* To whom correspondence should be addressed. Email [j.provis@sheffield.ac.uk](mailto:j.provis@sheffield.ac.uk),  
phone +44 114 222 5490, fax +44 114 222 5943

### **Abstract**

Irradiation is one of the characteristic conditions that nuclear wasteforms must withstand to assure integrity during their service life. This study investigates gamma irradiation resistance of an early age slag cement-based grout, which is of interest for the nuclear industry as it is internationally used for encapsulation of low and intermediate level radioactive wastes. The slag cement-based grout withstands a gamma irradiation dose of 4.77 MGy over 256 hours without reduction in its compressive strength; however, some cracking of irradiated samples was identified. The high strength retention is associated with the fact that the main hydration product forming in this binder, a calcium aluminum silicate hydrate (C-A-S-H) type gel, remains unmodified upon irradiation. Comparison with a heat-treated sample was carried out to identify potential effects of the temperature rise during irradiation exposure. The results suggested that formation of cracks is a combined effect of radiolysis and heating upon irradiation exposure.

**Keywords:** Radiation damage, cement, slag, grout, calcium silicate hydrate

## 1. Introduction

Cement grouts composed of blast furnace slag (BFS) and Portland cement (PC) are currently used for the encapsulation of intermediate and low level nuclear wastes in the UK<sup>1, 2</sup>. As these wasteforms are exposed to ionizing radiation throughout their lifetime, it is essential to understand the effects of radiation, and determine if they can withstand such service conditions. However, there is little information available in the literature regarding radiation effects on BFS-PC grouts, particularly when formulated with high replacement levels of PC by BFS. Most of the reported studies focus on hardened cements and concretes based solely on PC, which are used for nuclear safety and shielding structures in power plants, and assess the effects of gamma irradiation on mechanical properties and physical deterioration. Gamma irradiation is also the focus of the present study, being the most penetrating ionizing radiation and more difficult to shield than alpha or beta radiation.

PC consists of oxide clinker components (calcium silicates, aluminates and aluminoferrites) interground with gypsum, and upon hydration forms complex solid phases bound together by a gel-like phase referred to as calcium silicate hydrate (C-S-H), co-existing with other hydrated phases and an aqueous phase, also referred to as pore water<sup>3</sup>. The hydration of PC is an exothermic reaction and can generate a significant amount of heat, depending on the type and amount of clinker phases present in the PC. BFS, on the other hand, is a by-product of the iron-making industry rich in calcium aluminum silicates, whose reactivity is strongly dependent on its thermal history, particle size and amorphous fraction. BFS can behave in a similar manner to PC upon hydration, but it requires a more alkaline environment to dissolve, and thus promote the consequent formation of strength-giving phases. The high-volume addition of BFS to PC in cementitious grouts is favored in the nuclear waste encapsulation industry for several reasons including the significant reduction of the heat of hydration, a decreased amount of water required to achieve a workable cementitious grout that can be transferred into the canisters with the radioactive wastes<sup>4</sup>, and also for the reducing environment provided by the sulfide present in BFS, which could contribute to decreasing the mobility of some radionuclides<sup>1</sup>.

Soo and Milian<sup>5</sup> investigated the influence of the dose rate on the compressive strength of PC based materials at 10°C, identifying that the strength of the irradiated materials exposed to rather low dose rates (31 Gy/h) falls rapidly once the total dose exceeds about 0.1 MGy. Conversely, exposing the same materials to higher dose rates (380 kGy/h) led to an increase in mechanical strength, when exposed to a total dose of 10MGy. The mechanisms of cement strength loss due to radiation exposure are not well understood, but can be related to the loss of water from the cement hydrate components, which is described as radiolytic dehydration. However, if a moderate degree of heat is also generated or applied during irradiation, the kinetics of cement and slag hydration are accelerated, leading to a larger extent of reaction, which consequently promotes an increase in strength. This elucidates the complexity of understanding radiation effects in cementitious materials, as several phenomena will take place simultaneously, and depending on which one prevails in the system studied, it can lead to modification of the properties of the cement wasteform in different ways.

One of the main concerns related to the use of PC based grouts for the encapsulation of nuclear waste is the interaction of gamma rays with the water present in the pores of the hardened cement, which can induce hydrolysis of the water<sup>6</sup>. Bouniol et al.<sup>6</sup> stated that when the alkaline medium in concrete pores undergoes radiolysis, H<sub>2</sub> gas is produced as a primary product. As O<sub>2</sub> was not detected in their study, it was assumed that the other primary product of radiolysis was H<sub>2</sub>O<sub>2</sub>, which was mostly captured by the calcium present in the PC to form calcium peroxide octahydrate (CaO<sub>2</sub>.8H<sub>2</sub>O). This can then favor calcite (CaCO<sub>3</sub>) formation in the grout. Consistent with this, Vodak et al.<sup>7</sup> observed increased calcite formation in aged concrete samples exposed to high doses of gamma radiation, up to 1 MGy over 83 days. They also noted reductions in mechanical strength and pore volume. Bar-Nes et al.<sup>8</sup> also identified formation of calcium carbonates in gamma-irradiated PC samples, when exposed to 10 MGy for a period of 6 months.

In a later study, Vodak et al.<sup>9</sup> speculated that in addition to the effect of pore water radiolysis, the presence of micro-cracks due to radiolytic dehydration of the reaction products in the cement favors the ingress of CO<sub>2</sub> into the monolithic material, and its consequent reaction with the hydration products towards formation of calcium carbonates, especially at lower dose rates of radiation over a longer period of exposure. Conversely, higher total doses of gamma radiation, 130 to 836 MGy, were found to reduce the fraction of crystalline reaction

products formed during cement hydration, and even induced the decomposition of the cement clinker phases<sup>10</sup>.

It has also been reported that BFS-PC wasteforms<sup>11</sup> can show occasional spallation and cracking when irradiated at a dose rate of 10 kGy/h to a total dose of 6-9 MGy, with no identifiable variation in the reaction products. Richardson et al.<sup>12</sup> evaluated the microstructure of BFS-PC composites at a dose rate of 10 kGy/h to a total dose of 87 MGy over two years at 50°C. The formation of additional ettringite ( $\text{Ca}_6\text{Al}_2(\text{OH})_{12}(\text{SO}_4)_3 \cdot 26\text{H}_2\text{O}$ ) in the irradiated samples was observed when compared with the control samples, suggesting that gamma radiation may accelerate the oxidation of the sulfide ( $\text{S}^{2-}$ ) provided by the slag, to form sulfate,  $\text{SO}_4^{2-}$ , and promote further formation of ettringite. No alteration in the morphology and composition of the calcium silicate hydrate (C-S-H) was identified.

The present study investigates the gamma radiation resistance of a slag-based cement matrix with minimal inclusion of PC. An early-age BFS-PC grout (cured for only 8 days prior to irradiation) was selected as the basis of the study, as similar systems are used in the UK nuclear industry for encapsulation of LLW and ILW<sup>1</sup>. Irradiation effects at early age are of particular interest because the cement system has a significant amount of free water at this time, which can be subject to radiolysis and consequent  $\text{H}_2$  gas generation<sup>6</sup>. To investigate this effect, parallel samples were heat-treated for a length of time corresponding to the radiation exposure, and evaluated as a second control (in addition to unheated specimens) to distinguish the potential effects of elevated temperature from those associated solely with irradiation effects.

## 2. Experimental program

### 2.1. Materials

BFS from Redcar steel works, with a Blaine fineness of 286 m<sup>2</sup>/kg, was blended in a 9:1 ratio with Portland cement, CEM I (Hanson Ribblesdale) with a Blaine fineness of 385 m<sup>2</sup>/kg. The chemical compositions of BFS and PC are presented in Table 1. This blend of BFS and PC is referred as "binder" throughout this study.

**Table 1.** Composition of blast furnace slag (BFS) and Portland cement (PC), from X-ray fluorescence analysis. LOI is loss on ignition at 1000°C

Components as oxides (wt.%)	BFS	PC
CaO	38.8	65.4
SiO <sub>2</sub>	35.5	20.0
Al <sub>2</sub> O <sub>3</sub>	13.4	4.6
Fe <sub>2</sub> O <sub>3</sub>	0.9	3.1
MgO	7.6	2.1
K <sub>2</sub> O	0.4	0.7
Na <sub>2</sub> O	0.3	0.3
SO <sub>3</sub>	0.7	3.2
LOI	0.9	1.7
Others	1.5	0.6

## 2.2. Sample preparation

Hydrated paste samples were prepared at a water/binder ratio of 0.35. The pastes were manually mixed for 2 to 5 minutes, then mixed for 5 more minutes using a Whirl Mixer, and poured into 50 mL plastic centrifuge tubes, which were then sealed, and cured for 8 days at 20°C. After the curing period, the samples were de-molded, cut into cylinders 27 mm in diameter and 27 mm in height, and wrapped in aluminum foil. Samples were separated into three groups, each of which was treated in a specified environment prior to analysis:

- **Irradiated samples** were treated in the Dalton Cumbrian Facility with gamma radiation from a self-shielded <sup>60</sup>Co source. The specimens were irradiated in air at a dose rate of 18.6 kGy/h, to a total dose of 4.77 MGy over 256 h. The irradiation dose used in this study was selected considering that a total dose of 10 MGy is approximately equivalent to 100 years storage for an ILW wasteform <sup>13</sup>. Therefore the total dose used in this study corresponds to the conditions a cementitious wasteform must withstand during the anticipated period of interim storage prior to geological disposal.

- **Control samples** were kept at 20°C in the lab for a time equivalent to the irradiation period before testing.
- **Heated samples** were kept at 50°C in air, using an electric oven, for a time equivalent to the irradiation period before testing. This temperature was specified to match the average temperature of  $50 \pm 5^\circ\text{C}$  in the irradiation chamber during the radiation exposure.

### 2.3 Tests and analysis

Sections of each monolithic specimen were immersed in acetone (to arrest the hydration reaction process) and retained for microscopic analysis, while the remaining material was crushed and then immersed in acetone. After 3 days, the samples were removed from the acetone, dried, and kept in sealed containers to avoid carbonation during storage. Samples were then analyzed:

- X-ray diffraction (XRD) was conducted using a Siemens D5000 instrument ( $\text{Cu K}_{\alpha 1}$ ,  $\lambda = 1.54178 \text{ \AA}$ ), with a step size of  $0.02^\circ$  and a scanning speed of  $0.5^\circ/\text{min}$ .
- Solid-state  $^{29}\text{Si}$  MAS NMR spectra were collected at 59.56 MHz on a Varian Unity Inova 300 (7.05 T) spectrometer using a probe for 7.5 mm o.d. zirconia rotors and a spinning speed of 5 kHz. The  $^{29}\text{Si}$  MAS NMR employed a  $90^\circ$  pulse duration of 5  $\mu\text{s}$ , a relaxation delay of 5 s, and 14000 scans. Solid-state  $^{27}\text{Al}$  MAS NMR spectra were acquired at 104.198 MHz, using a Varian VNMRS 400 (9.4T) spectrometer and a probe for 4 mm o.d. zirconia rotors, a spinning speed of 14 kHz with a pulse width of 1  $\mu\text{s}$  (approximately  $25^\circ$ ), a relaxation delay of 0.2 s, and a minimum of 7000 scans.  $^{29}\text{Si}$  and  $^{27}\text{Al}$  chemical shifts are referenced to external samples of tetramethylsilane (TMS) and a 1.0 M aqueous solution of  $\text{Al}(\text{NO}_3)_3$ , respectively.
- Thermogravimetric analysis (TGA) was carried out using a Perkin Elmer Pyris 1 TGA. Approximately 40 mg of each sample was weighed, placed and heated at  $10^\circ\text{C}/\text{min}$  in an alumina crucible under a nitrogen atmosphere.
- Microscopic inspection of solid samples was carried out using an optical microscope Nikon Eclipse LV150 with  $50\times$  magnification, with Buehler Omnimet Enterprise 9.5

software, to identify any large cracks forming in the specimens. Thresholding of the micrographs was carried out using ImageJ.

Compressive strength of cylindrical specimens was measured using a Zwick Roell Z050 machine. The cross head speed was 0.5mm/min, and the results were corrected with a shape factor of 0.85 for cylinders of aspect ratio 1.0.

### 3. Results and discussion

#### 3.1. X-ray diffraction

Figure 1 illustrates the X-ray diffractograms of the studied samples compared with the anhydrous 9:1 BFS-PC powder. The anhydrous mix is predominantly poorly crystalline due to the large fraction of slag present. Reflection peaks of crystalline åkermanite ( $\text{Ca}_2\text{MgSi}_2\text{O}_7$ , powder diffraction file, PDF, #076-0841), contributed by the slag, were also identified along with the PC clinker phases alite ( $\text{Ca}_3\text{SiO}_5$ , PDF #031-0301) and belite ( $\beta\text{-Ca}_2\text{SiO}_4$ , PDF #031-0299). Upon initial hydration and following subsequent treatments, all samples showed a clear reduction in the intensity of the reflections assigned to the clinker phases, suggesting that a significant amount of the PC has already reacted.

A small peak at  $11.3^\circ$   $2\theta$  was observed in all samples, assigned to a hydrotalcite ( $\text{Mg}_6\text{Al}_2(\text{CO}_3)(\text{OH})_{16}\cdot 4\text{H}_2\text{O}$ , PDF #89-0460) with a layered double hydroxide structure. This phase is commonly formed in slag-rich PC blends and alkali-activated slags, when the slag has a moderate to high MgO content (> 5 wt.% MgO in the slag)<sup>14</sup>. A poorly crystalline calcium silicate hydrate (C-S-H) phase is identified as the main hydration product, according to the broad peak centered at  $29^\circ$   $2\theta$ . This phase is derived from the reaction of both BFS and PC. Reflections assigned to portlandite ( $\text{Ca}(\text{OH})_2$ , PDF #-044-1481), one of the main products of PC hydration, were also observed along with traces of calcite ( $\text{CaCO}_3$ , PDF #005-0586).

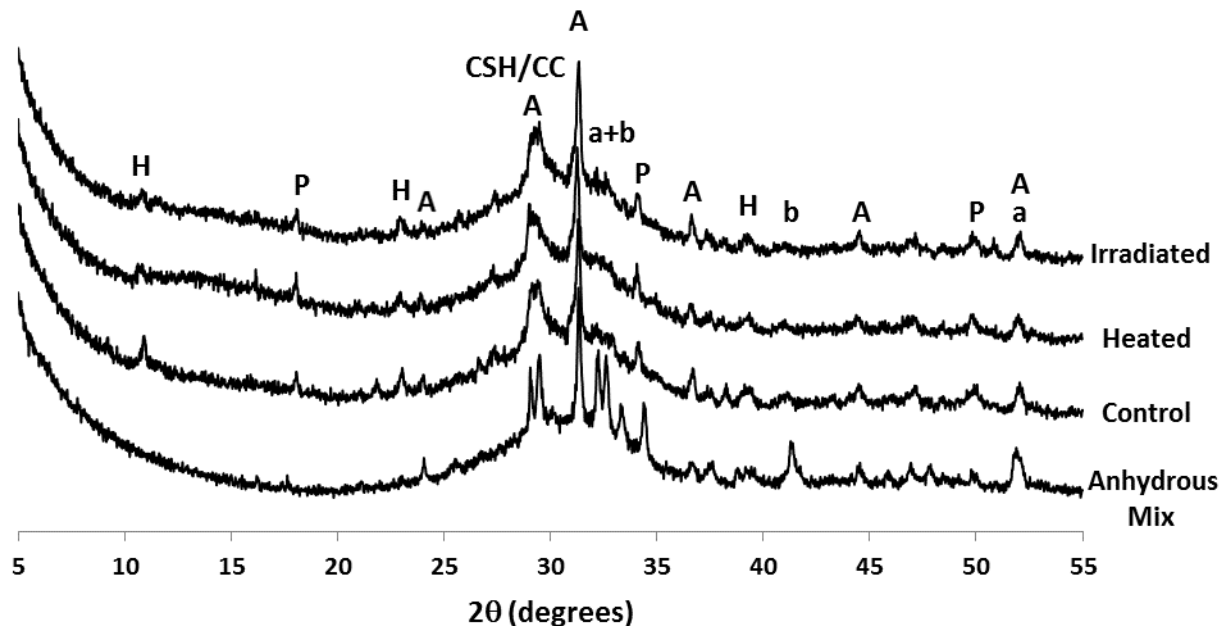


**Figure 1.** X-ray diffractograms of anhydrous BFS-OPC powder and the samples studied. Peaks marked are åkermanite (A), calcite (CC), hydrotalcite (H), portlandite (P), alite (a), belite (b) and calcium silicate hydrate (CSH).

The XRD pattern for the irradiated sample shows no significant difference from those of the other specimens analyzed, suggesting that the crystalline reaction products formed at this early stage of hydration are able to withstand gamma irradiation exposure. This is in accordance with the observations made for similar systems at different ages, where a slightly lower dose rate (10 kGy/h) compared with the present study (18.6 kGy/h) was applied<sup>11, 12</sup>. The formation of crystalline ettringite (main reflection at  $9.09^\circ 2\theta$ ) was not observed in our samples, conversely to the results identified by Richardson et al.<sup>12</sup>, which might be a consequence of the difference in age of the materials evaluated, or may indicate that this phase is not sufficiently ordered to enable its identification by XRD. The possible presence of ettringite in the samples assessed will be discussed in more detail below.

### 3.2. Solid state $^{27}\text{Al}$ and $^{29}\text{Si}$ MAS NMR spectroscopy

Figure 2 shows the  $^{27}\text{Al}$  MAS NMR spectra of the anhydrous mix and the hydrated samples studied.  $^{27}\text{Al}$  MAS NMR spectra of minerals and glasses typically show three distinct aluminum coordination environments ( $\text{Al}^{(\text{IV})}$ ,  $\text{Al}^{(\text{V})}$  and  $\text{Al}^{(\text{VI})}$ ), which are located at chemical

shifts between 50 to 80 ppm, 30 to 50 ppm and -10 to 30 ppm, respectively<sup>15</sup>. The anhydrous mix presents a broad resonance between 40 and 80 ppm centered around 60 ppm that cannot be attributed to a sole aluminum environment, and corresponds to the glassy fraction which comprises the majority of the BFS, as identified in the XRD data for the anhydrous BFS-PC mix (Fig 1).

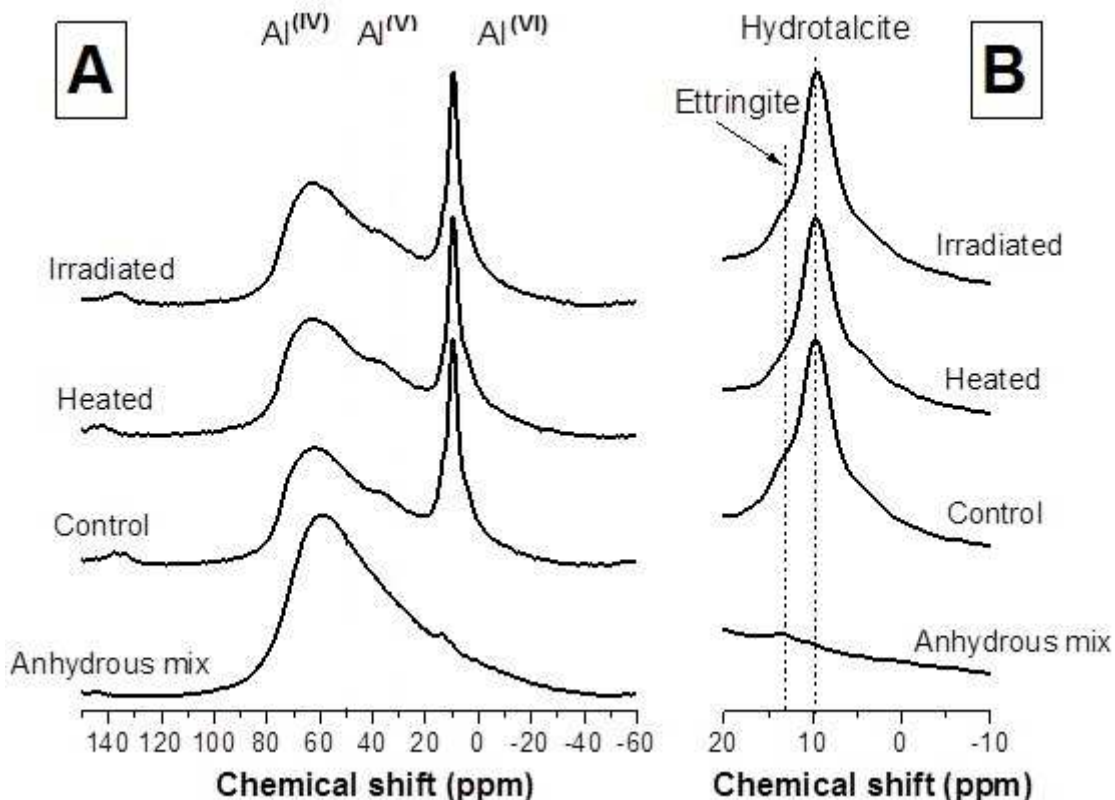


**Figure 2.** Solid-state  $^{27}\text{Al}$  MAS NMR spectra of (A) the anhydrous BFS-PC powder mix and the samples studied, and (B) enlargement of the  $\text{Al}^{(\text{VI})}$  region of the spectra

Upon hydration, a high intensity band in the  $\text{Al}^{(\text{VI})}$  region, centered at 9.5 ppm, is identified. This resonance is assigned to the hydrotalcite type phase<sup>16</sup> which was identified by XRD (Fig 1). A low intensity, but well resolved, shoulder centered at 13 ppm is also observed in the control sample. A band at this chemical shift corresponds to ettringite<sup>17</sup>, confirming the formation of this phase in the early age BFS-PC evaluated in this study, even though it was not identified by XRD.

In the  $\text{Al}^{(\text{IV})}$  region a significant contribution of the remnant unreacted slag is observed; however, the line shape of this band differs from that observed in the anhydrous mix. This

indicates the potential overlap of resonances assignable to hydration reaction products containing tetrahedral aluminum environments, in particular an aluminum-substituted C-S-H type phase. Such a phase is typically identified as the dominant reaction product of BFS-OPC grouts, and its Al is present in tetrahedral coordination<sup>18</sup>.

In the heat-treated samples, similar resonances to those observed in the control sample are identified, however, the shoulder assigned to ettringite is not observed. This indicates that the heat treatment adopted in this study is sufficient to promote the full dehydration and potential decomposition of this hydrated phase, consistent with the known instability of ettringite at temperatures around 50°C<sup>19</sup>.

However, in the irradiated sample (which has also been held at 50°C throughout irradiation), the ettringite resonance is still observable, although slightly less intense than in the control sample. This indicates that the irradiation is stabilizing the ettringite in spite of the heating conditions reached during the irradiation exposure, consistent with the observations of Richardson et al.<sup>12</sup> in older BFS-PC grout specimens. The stability of ettringite is strongly dependent on temperature and the concentration of SO<sub>4</sub><sup>2-</sup>, so that higher concentrations of sulfates are required for its precipitation at increased temperatures<sup>20</sup>. Richardson et al.<sup>12</sup> proposed that radiolytic oxidation of the sulfides from the BFS to sulfates is likely to take place in this type of grout, and this increased concentration of sulfates is then sufficient to stabilize ettringite under the temperature conditions reached upon gamma radiation exposure. This explains why ettringite is not observed in the heat-treated samples, where there is no mechanism to induce oxidation of sulfides. The stability of ettringite upon irradiation is of particular importance for the immobilization of nuclear wastes in cements, as this phase can chemically bind different radionuclides via ion exchange mechanisms<sup>21</sup>. The Al environments in the hydrotalcite-type and C-S-H type phases are also seen to remain largely unchanged during irradiation, and these are also important contributors to the retention of radionuclides within these wasteforms.

The <sup>29</sup>Si MAS NMR spectra of the BFS-PC specimens are shown in Fig 3. The unreacted BFS-PC blend has two broad but distinctive resonances centered at -71 ppm and -74 ppm, assigned to the PC phase belite<sup>22</sup>, as identified by XRD (Fig 1), and the åkermanite present in the anhydrous slag<sup>15</sup>. These bands remain in the hydrated samples, although with a

reduced intensity, indicating that a significant fraction of unreacted material is still present in these cements, consistent with the early age of the cementitious grouts studied here. Upon hydration, new bands centered at -81 ppm and -85 ppm are observed, and these are assigned to the Q<sup>2</sup>(1Al) and Q<sup>2</sup> sites typically identified in C-A-S-H type products <sup>23</sup>. This confirms that even at early ages of curing, the main binding phase forming in the BFS-PC grout is an Al-substituted C-S-H (C-A-S-H) product. Very similar resonances are identified in the heat-treated and irradiated samples, indicating that notable changes are not taking place in the aluminosilicate chains composing the C-A-S-H phase in this system, and therefore it is concluded that this phase can withstand gamma irradiation exposure. These results are in good agreement with those reported by Richardson et al. <sup>12</sup>, where the Si environments in the C-S-H type phase remained unchanged after 2 years of irradiation and a total dose of 84 MGy.

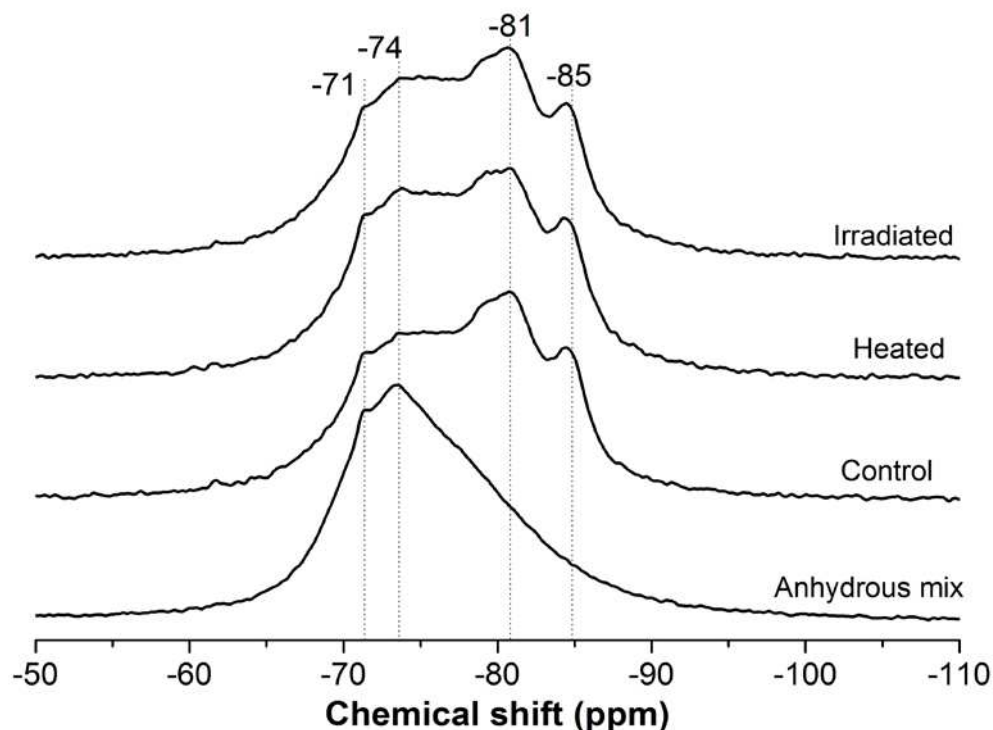


**Figure 3.** <sup>29</sup>Si MAS NMR spectra of anhydrous BFS-PC powder mix, and the samples studied

### 3.3. Thermogravimetric analysis

Figure 4 shows the thermograms and differential thermograms of the samples studied. Differences among the samples can be observed below 100°C (inset, Fig 4B), associated with the release of free water from the specimens and the initial dehydration of the C-S-H phase<sup>24</sup>. The distinctive mass loss at 80°C is attributed to the removal of physisorbed water in hydrotalcite<sup>25</sup>. The mass loss up to 100°C was 5.9 % for the irradiated sample, and 5.5 % for the heated sample, being smaller than that of the control sample (7.6 %), indicating a reduced content of free water in the irradiated and heated specimens. Above 100°C, all samples show very similar profiles of mass loss, with the minor mass loss at 130°C assigned to dehydration of ettringite<sup>24</sup>, and at 440°C attributed to the dehydroxylation of the brucite layers in hydrotalcite<sup>25</sup>. The measured mass loss from 100°C to 1000°C was 7.4 % for the irradiated sample, 7.0 % for the heated sample and 7.7 % for the control. This is consistent with the report of Pottier and Glasser<sup>11</sup> for irradiated BFS-PC specimens, in which there are no major changes observed by thermal analysis in irradiated samples compared with control specimens.

The slightly higher weight loss identified by TGA in the irradiated samples, compared with the heated specimens, may suggest that the irradiation is inducing either a slightly higher extent of hydration of the BFS-OPC grout, or less desiccation of the hydration products present in this cement while being held at a corresponding temperature for the same duration.

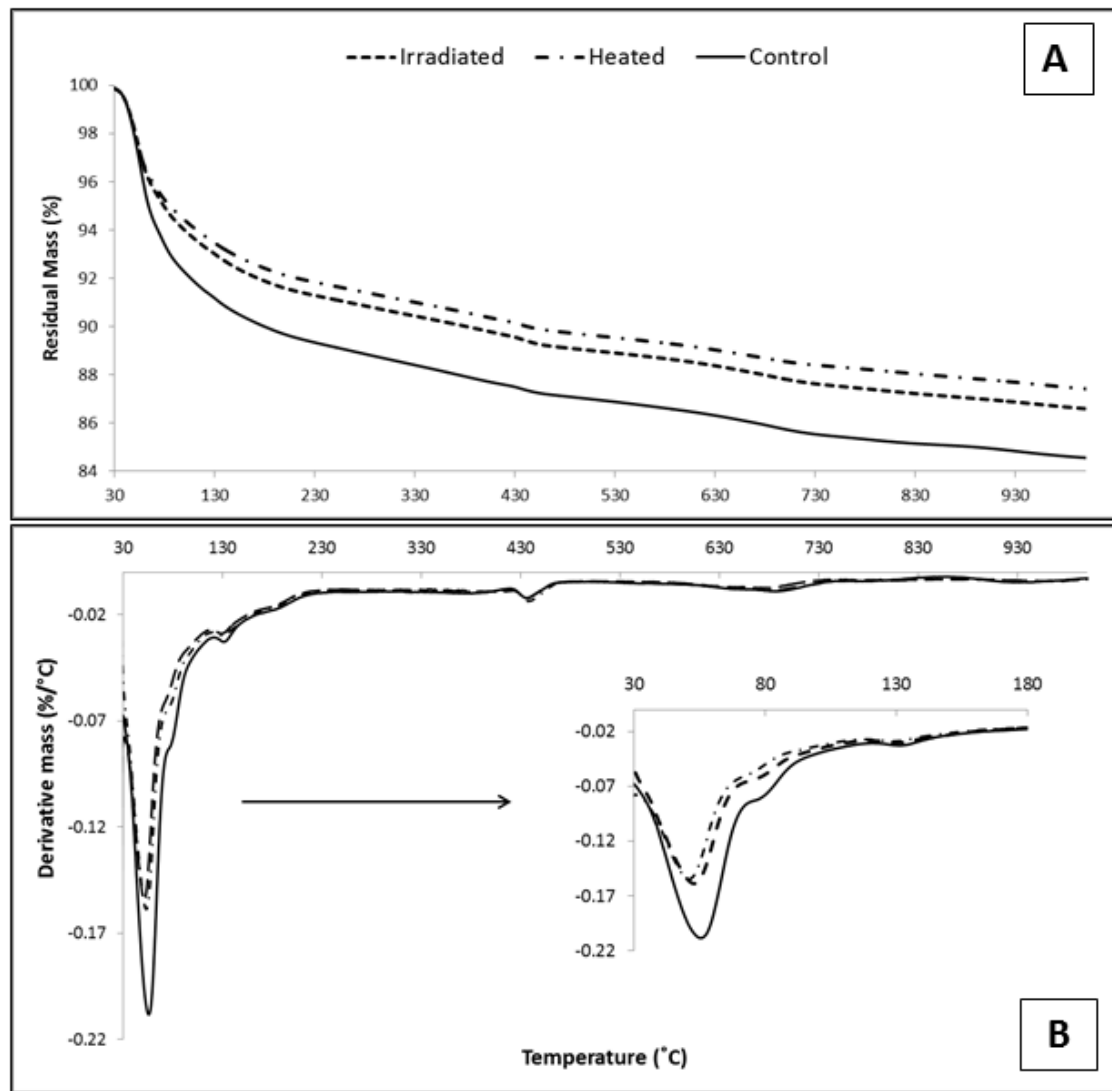


**Figure 4.** Thermograms (A) and differential thermograms (B) (mass loss downwards) of the control, heated and irradiated BFS:PC samples

The mass loss associated with the presence of calcium carbonate polymorphs appears at 500–800°C<sup>26</sup>. The differential thermogram profile of the irradiated sample did not show any significant differences in this region compared with the heated and control specimens. Although formation of calcium carbonates by chemical reaction of atmospheric CO<sub>2</sub> with the calcium rich phases in cements, referred to as carbonation, has been reported for neat PC samples upon gamma irradiation<sup>7</sup>, it appears that irradiation of an early age BFS-PC specimen does not favor carbonation. It has been reported<sup>27</sup> that the irradiation causes the formation of calcium peroxide octahydrate in irradiated PC paste through the interaction between Ca(OH)<sub>2</sub> and the H<sub>2</sub>O<sub>2</sub> produced via radiolysis, which promotes carbonation. The BFS-PC grout evaluated here has only 10 wt.% PC, thus the majority of the Ca(OH)<sub>2</sub> formed

during the hydration of PC is consumed by reaction with the BFS<sup>18</sup>, reducing the probability of calcium peroxide octahydrate formation, and consequently minimizing the susceptibility to carbonation of the blended grouts upon gamma irradiation.

### **3.4. Microscopic inspection**

Figure 5 presents optical micrographs, and the corresponding thresholded images, showing pores (in black) and solid regions (in white) of the samples evaluated. The relatively large pores observed in all the samples are likely to be associated with the air which is entrapped during mixing and paste casting. It is clear from the images that the irradiated sample (I) has more open pores and cracks compared with the heated (H) and control (C) samples, in good agreement with the literature for similar samples at later age<sup>11</sup>. As discussed in the previous section, both the irradiated and heated samples had reduced weight loss at temperatures below 100°C compared with the control sample. Although the level of water reduction caused by the irradiation and by the heat-treatment was similar, the dehydration mechanisms in these treatments appear to be different, resulting in the different observed degrees of cracking. Pottier and Glasser<sup>11</sup> explained the process of microcrack formation upon irradiation of cement grouts as being a consequence of pressurization of the radiolytic gases inside the cement matrix, and the results presented here are consistent with their analysis.

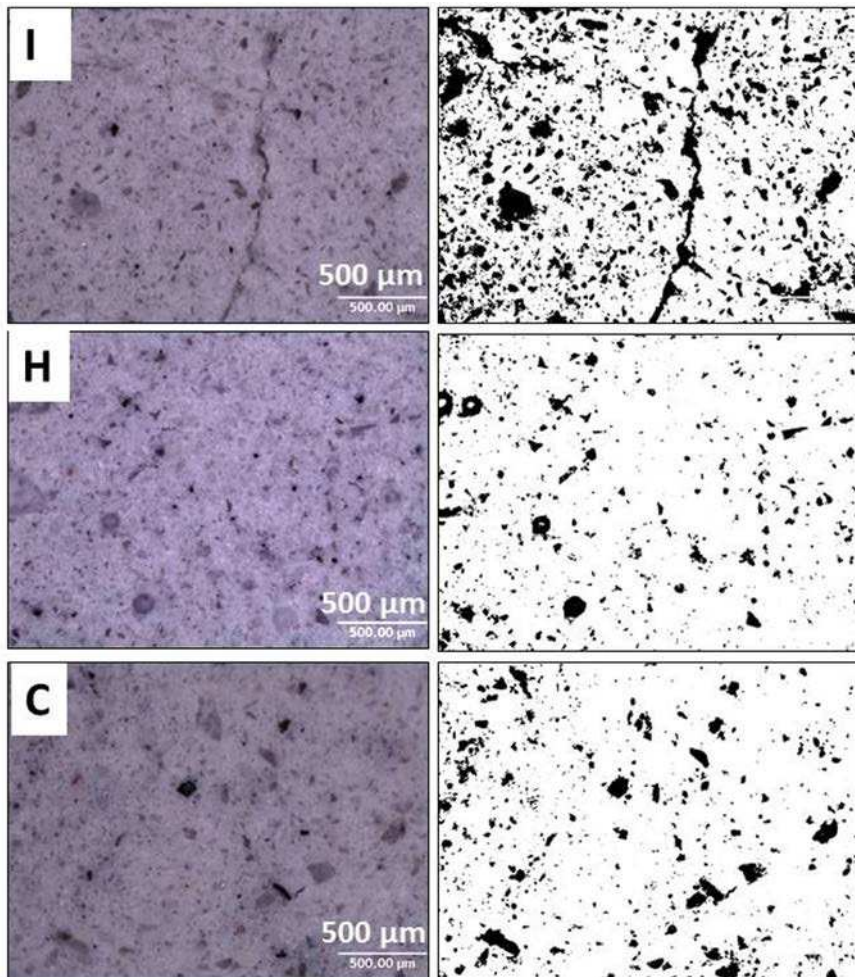


**Figure 5.** Optical micrographs of (I) irradiated, (H) heated and (C) control samples, and corresponding thresholded images showing pore and solid regions

### 3.5. Compressive strength

Figure 6 shows the compressive strengths of the samples studied. The compressive strength of the heated sample is 7 % higher than that of the control, which is within the experimental error. However, the irradiated sample exhibited an increase of 19 % in compressive strength compared with the control grout. An increased strength in irradiated cements was also observed in a PC based system <sup>28</sup>. However, this trend differs from that which has been identified in PC cured at high temperatures, where reductions in compressive strength have been reported as curing temperature increases. Gallucci et al. <sup>29</sup> identified significant changes in the microstructure of C-S-H phase in cements depending on the temperature of curing, so that increased polymerization and apparent densification of this phase was observed upon

curing at 60°C, compared with samples cured at 25°C. This apparent increase in the density of C-S-H was associated with a decrease in the amount of structural water in this binding phase, when forming at high temperatures of curing, leading to a coarser and more porous microstructure, which induces reductions in compressive strength.

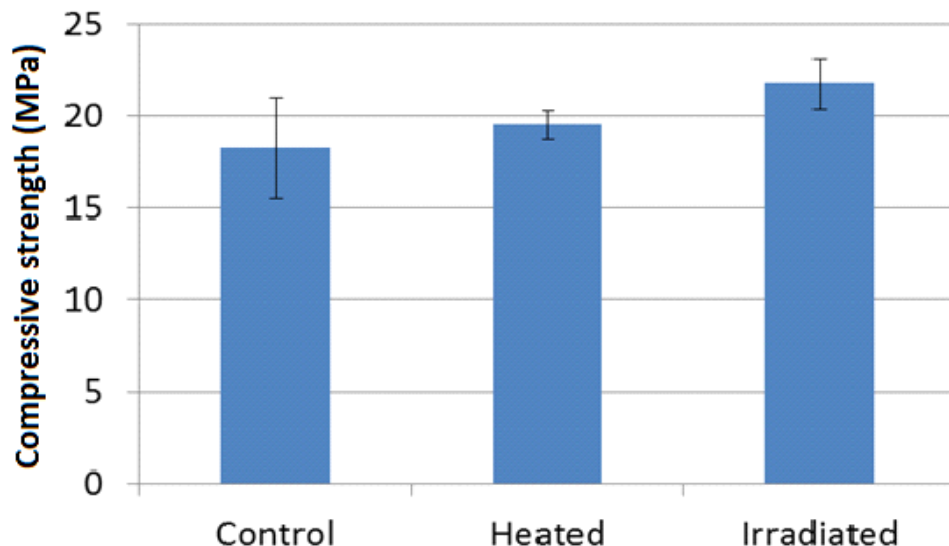


**Figure 6.** Compressive strength of BFS:PC pastes. Error bars show one standard deviation of three measurements

Further investigation is required to elucidate the mechanisms leading to the strength development of irradiated cementitious grouts. It may be that the stabilization of ettringite (which is a highly voluminous phase) contributed in a significant way to increase the strength of the irradiated specimens, but this cannot yet be confirmed. The results show that the early age BFS-PC system retains, and in fact improves, its mechanical strength upon irradiation, even though cracks and increased porosity were observed post-irradiation.

#### 4. Conclusions

The effects of gamma radiation and heat on a BFS-PC composite cement at early age were studied. The crystalline phases presented in the system were able to withstand the dose rate and total degree of gamma irradiation tested in the present study (4.77 MGy over 256 h),

without notable modifications; the irradiated samples retained ettringite in their structure, which was present at 20°C but not when specimens were heated at 50°C (corresponding to the temperature in the irradiation chamber) for a length of time equal to the duration of irradiation. The Si and Al environments in the C-S-H type gel and secondary hydrate phases retained stability upon irradiation. Irradiation-induced carbonation, previously reported for PC-based systems, was not identified in the specimens evaluated here. The reduced amount of Ca(OH)<sub>2</sub> in the system, owing to the small amount of PC used, appears to have minimized the formation of calcium peroxide octahydrate which is an important intermediate in the radiation-induced carbonation process.

This result demonstrates that the replacement of PC by BFS can modify the performance of the cement matrix under irradiation exposure. Gamma radiation caused a reduction in the content of physically bonded water within the binder, resulting in microcracking. Although exposure to 50°C also caused a comparable level of water reduction in the grout, microcracks were not observed in that sample, which elucidates that the elevated temperature in the radiation chamber is not the main cause of the microcracks. The dehydration mechanisms in these two environments appear to be different, resulting in the different microstructures. Gamma irradiation also increased the compressive strength of the cement despite the increased porosity and microcracks, which may be due to enhancements in curing and/or the densification of the material.

## **5. Acknowledgements**

This study has been sponsored by EPSRC through the University of Sheffield/University of Manchester Doctoral Training Centre ‘Nuclear FiRST’. The NMR spectra were collected using the EPSRC UK National Solid-state NMR Service at Durham University, and the assistance of Dr David Apperley is gratefully acknowledged. Special thanks are due to Dr Ruth Edge and Dalton Cumbrian Facility for their great assistance in the irradiation experiments.

## **5. References**

1. M. Atkins and F.P. Glasser: Application of Portland cement-based materials to radioactive waste immobilization. *Waste Manag.* **12**(2), 105 (1992).
2. J.H. Sharp, J. Hill, N.B. Milestone and E.W. Miller: Cementitious systems for encapsulation of intermediate level waste, in Proceedings 9<sup>th</sup> International Conference on Radioactive Waste Management and Environmental Remediation, (2003), p. 21.
3. P.C. Hewlett: Lea's Chemistry of Cement and Concrete, 4th Ed. (Elsevier, 1998).
4. M.I. Ojavan and W.E. Lee: An introduction to nuclear waste immobilisation (Elsevier, 2005). pp. 179-200.
5. P. Soo and L. Milian: The effect of gamma radiation on the strength of Portland cement mortars. *J. Mat. Sci. Lett.* **20**(14), 1345 (2001).
6. P. Bouniol and A. Aspart: Disappearance of oxygen in concrete under irradiation: the role of peroxides in radiolysis. *Cem. Concr. Res.* **28**(11), 1669 (1998).
7. F. Vodák, K. Trtík, V. Sopko, O. Kapičková and P. Demo: Effect of  $\gamma$ -irradiation on strength of concrete for nuclear-safety structures. *Cem. Concr. Res.* **35**(7), 1447 (2005).
8. G. Bar-Nes, A. Katz, Y. Peled and Y. Zeiri: The combined effect of radiation and carbonation on the immobilization of Sr and Cs ions in cementitious pastes. *Mater. Struct.* **41**, 1563 (2008).
9. F. Vodák, V. Vydra, K. Trtík and O. Kapičková: Effect of gamma irradiation on properties of hardened cement paste. *Mater. Struct.* **44**(1), 101 (2011).
10. A. Lowinska-Kluge and P. Piszora: Effect of gamma irradiation on cement composites observed with XRD and SEM methods in the range of radiation dose 0-1409 MGy. *Acta Phys. Pol. A.* **114**(2), 399 (2008).
11. P.E. Pottier and F.P. Glasser: Characterization of low and medium-level radioactive waste forms. Final report-2<sup>nd</sup> Programme 1980-84, (Commission of the European Communities, Luxembourg, 1986).
12. I. Richardson, G. Groves and C. Wilding: Effect of  $\gamma$ -radiation on the microstructure and microchemistry of GGBFS/OPC cement blends, in *MRS Proceedings*, (176, Cambridge Univ Press, 1989), p. 31.
13. S. Curwen and F. Ridley: Generic report on the properties of BFS/OPC and PFA/OPC as encapsulation matrices for ILW, PETF (89) P40, BNFL (Research and Development Department Sellafield, 1989), 66 pp..
14. S.A. Bernal, R. San Nicolas, R.J. Myers, R. Mejía de Gutiérrez, F. Puertas, J.S.J. van Deventer and J.L. Provis: MgO content of slag controls phase evolution and structural changes induced by accelerated carbonation in alkali-activated binders. *Cem Concr Res.* **57**, 33 (2014).
15. R.J. Kirkpatrick: MAS NMR-Spectroscopy of minerals and glasses. *Rev. Mineral.* **18**, 341 (1988).
16. K.J.D. MacKenzie, R.H. Meinholt, S. B.L. and Z. Xu:  $^{27}\text{Al}$  and  $^{25}\text{Mg}$  solid-state magic-angle spinning nuclear magnetic resonance study of hydrotalcite and its thermal decomposition sequence. *J. Mater. Chem.* **3**(12), 1263 (1993).
17. M.D. Andersen, H.J. Jakobsen and J. Skibsted: A new aluminium-hydrate species in hydrated Portland cements characterized by  $^{27}\text{Al}$  and  $^{29}\text{Si}$  MAS NMR spectroscopy. *Cem. Concr. Res.* **36**(1), 3 (2006).
18. R. Taylor, I.G. Richardson and R.M.D. Brydson: Composition and microstructure of 20-year-old ordinary Portland cement-ground granulated blast-furnace slag blends containing 0 to 100% slag. *Cem. Concr. Res.* **40**(7), 971 (2010).

19. B. Lothenbach, T. Matschei, G. Möschner and F.P. Glasser: Thermodynamic modelling of the effect of temperature on the hydration and porosity of Portland cement. *Cem. Concr. Res.* **38**(1), 1 (2008).
20. R. Barbarulo, H. Peycelon and S. Prene: Experimental study and modelling of sulfate sorption on calcium silicate hydrates. *Ann. Chim.- Sci. Mat.* **28**, S5 (2003).
21. N.D.M. Evans: Binding mechanisms of radionuclides to cement. *Cem. Concr. Res.* **38**(4), 543 (2008).
22. S.L. Poulsen, V. Kocabă, G. Le Saoût, H.J. Jakobsen, K.L. Scrivener and J. Skibsted: Improved quantification of alite and belite in anhydrous Portland cements by <sup>29</sup>Si MAS NMR: Effects of paramagnetic ions. *Solid State Nucl. Mag.* **36**(1), 32 (2009).
23. M.D. Andersen, H.J. Jakobsen and J. Skibsted: Incorporation of aluminum in the calcium silicate hydrate (C-S-H) of hydrated Portland cements: A high-field <sup>27</sup>Al and <sup>29</sup>Si MAS NMR investigation. *Inorg. Chem.* **42**(7), 2280 (2003).
24. L. Alarcon-Ruiz, G. Platret, E. Massieu and A. Ehrlacher: The use of thermal analysis in assessing the effect of temperature on a cement paste. *Cem. Concr. Res.* **35**(3), 609 (2005).
25. M. Mokhtar, A. Inayat, J. Ofili and W. Schwieger: Thermal decomposition, gas phase hydration and liquid phase reconstruction in the system Mg/Al hydrotalcite/mixed oxide: a comparative study. *Appl. Clay Sci.* **50**(2), 176 (2010).
26. G. Villain, M. Thiery and G. Platret: Measurement methods of carbonation profiles in concrete: thermogravimetry, chemical analysis and gammadensimetry. *Cem. Concr. Res.* **37**(8), 1182 (2007).
27. P. Bouniol and E. Bjergbakke: A comprehensive model to describe radiolytic processes in cement medium. *J. Nucl. Mater.* **372**(1), 1 (2008).
28. B. Nowakowski: Influence of penetrating ionizing radiation on the curing of grouts and cement mortars. *Build. Sci.* **7**(4), 271 (1972).
29. E. Gallucci, X. Zhang and K. Scrivener: Effect of temperature on the microstructure of calcium silicate hydrate (C-S-H). *Cem. Concr. Res.* **53**(185-195), (2013).